

5-2017

Fatigue Analysis of the Greenup Lock Gate on the Ohio River

Maggie Langston

Follow this and additional works at: <http://scholarworks.uark.edu/cveguht>



Part of the [Civil Engineering Commons](#), and the [Structural Engineering Commons](#)

Recommended Citation

Langston, Maggie, "Fatigue Analysis of the Greenup Lock Gate on the Ohio River" (2017). *Civil Engineering Undergraduate Honors Theses*. 36.

<http://scholarworks.uark.edu/cveguht/36>

This Thesis is brought to you for free and open access by the Civil Engineering at ScholarWorks@UARK. It has been accepted for inclusion in Civil Engineering Undergraduate Honors Theses by an authorized administrator of ScholarWorks@UARK. For more information, please contact ccmiddle@uark.edu, drowens@uark.edu, scholar@uark.edu.

Fatigue Analysis of the Greenup Lock Gate on the Ohio River

Maggie B. Langston

Undergraduate Honors Thesis
Program in Civil Engineering
University of Arkansas
Spring 2017

Research Advisor: Dr. Gary Prinz
University of Arkansas
prinz@uark.edu

Abstract

This thesis analyzes damage due to fatigue of a typical lock gate on the United States waterway transportation system. Functioning lock gates are essential for this mode of transportation because they control water levels and provide access through dams for ships. Fatigue cracking is caused by cyclic loading and corrosion. Cyclic loading on a lock gate was imitated using a finite element model. This model was used to calculate stress ranges for a cycle so that the number of cycles to failure could be calculated. The proportion of cycles to cycles to failure is known as the fatigue capacity. A linear fatigue damage accumulation rule (Miner's Rule) helped determine the fatigue critical regions within the gate. Twenty-seven sections of high stress were identified and analyzed. A section at the base of the lock gate sustained the most damage and was determined to be the most fatigue susceptible location. Further analysis and experimentation will validate these results so that retrofits become a possibility in preventing damage due to fatigue caused by cyclic loading.

1. Introduction

Waterway transportation is an important mode of transportation for industry in the United States. In 2015, over 900 million short tons were transported using waterways (WCSC, 2015). That amount of cargo is equivalent to 36 million standard semi-trailer trucks carrying their maximum capacity of 25 short tons, allowed by the Federal Highway Administration (Transportation Research Board and National Research Council, 2010), (AHTD, 2015). All this cargo relies on the 191 lock sites and 236 lock chambers that operate in dams along the rivers of the United States (USACE, 2013). The lock gates in these dams are essential to the waterway transportation system due to their ability to adjust water levels. Lock gates open for ships to enter the chamber, close while the water level changes, and open back up so that ships can continue along the river, see Figure 1.

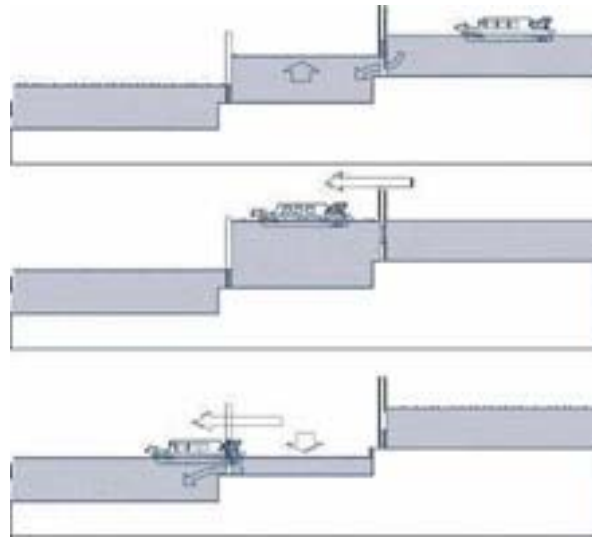


Figure 1. Lock Gate Operation Diagram

Most of these gates were built in the early to mid 20th century and were designed with a lifespan of 50 years (ASCE, 2017). The gates are reaching and exceeding their design lives leading to an increased need in repairs. Repairs exist but are costly due to their debilitating effect on commerce (Baker, 2004). One lock system, the Greenup Locks and Dam, cost approximately \$14

million in “direct tow-operating costs to industry just sitting idle in back-ups” from having an unscheduled maintenance closure of five weeks (Grier, 2009).

Unfortunately, the gates that allow this access and regulation are experiencing fatigue cracks. Fatigue cracks occur due to cyclic loading. The lock gate goes through a cycle of loading every time the water levels are adjusted. Fatigue cracking due to cyclic loading is compounded by the amount of environmental exposure the gates encounter. Exposure to sun, wind, and water, especially, leads to corrosion which weakens the gates making them more susceptible to fatigue cracks.

2. Objectives and Scope

The objective of this research project is to identify critical fatigue regions within typical components of a lock gate. A specific lock gate, the Greenup Locks and Dam on the Ohio River, was chosen by the US Army Corps of Engineers to coincide with a scheduled dewatering of a lock and the research project’s proposed schedule. A finite element analysis of the lock gate was performed to assist with the stress analysis due to the complex geometry of the gate.

3. Method

3.1 Finite Element Analysis

A finite element model was developed, by others, using ABAQUS 6.14 and the plans from the Greenup Locks and Dam on the Ohio River. The model gives a general estimate of where high stress areas are located so that damage due to fatigue can be estimated.

3.1.1 Modeling the Lock Gate

Finite element models use a combination of elements, nodes, and boundary conditions to imitate a structure. An element is created when nodes are connected. The more nodes that make an element, the more accurate that element will be. Therefore, four nodes were connected to make

a single element in this model. Nodes are points that have coordinates and boundary conditions. Boundary conditions limit movement like support connections.

One door of the specific lock gate was modeled due to symmetry. Its dimensions are 63.5 feet by 61.5 feet by 5.71 feet, see Figure 2. After the model was designed, hydrostatic loads with amplification factors were applied to simulate the changing water pressures on the gate, see Figure 3. The water pressure on the back of the gate remained constant while it varied on the front to simulate the water level changing for one lockage (the process of raising or lowering water levels to allow passage through a lock).

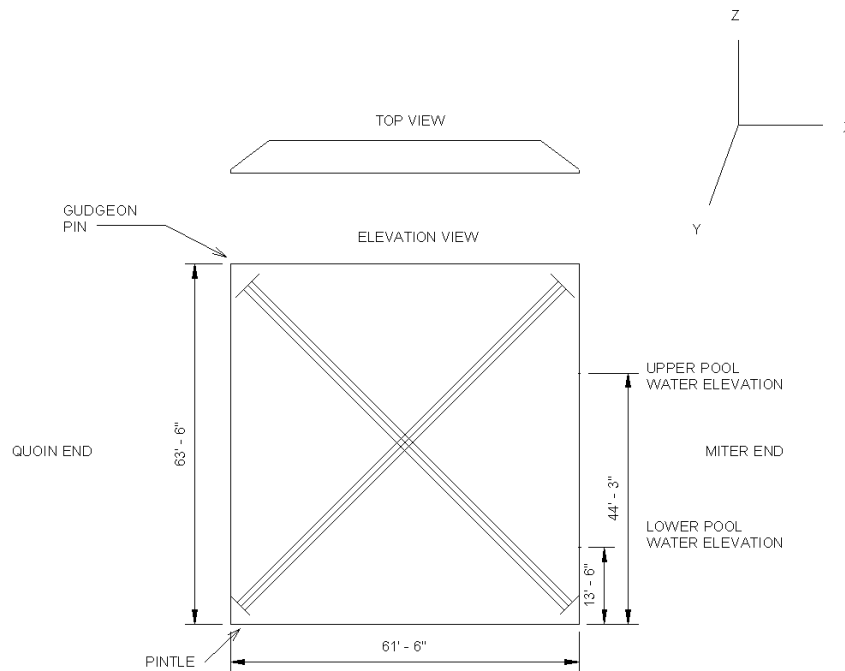


Figure 2. Upstream Elevation and Top View of Miter Gate

The loads were applied in three separate steps. Gravity was applied in the first step and propagated to steps 2 and 3. The constant high level load on the downstream face of the gate was applied in the second step and propagated to the third step. The third step was split into 60 time-step intervals with different load heights applied to simulate the raising and lowering of the water's level on the upstream face of the gate.

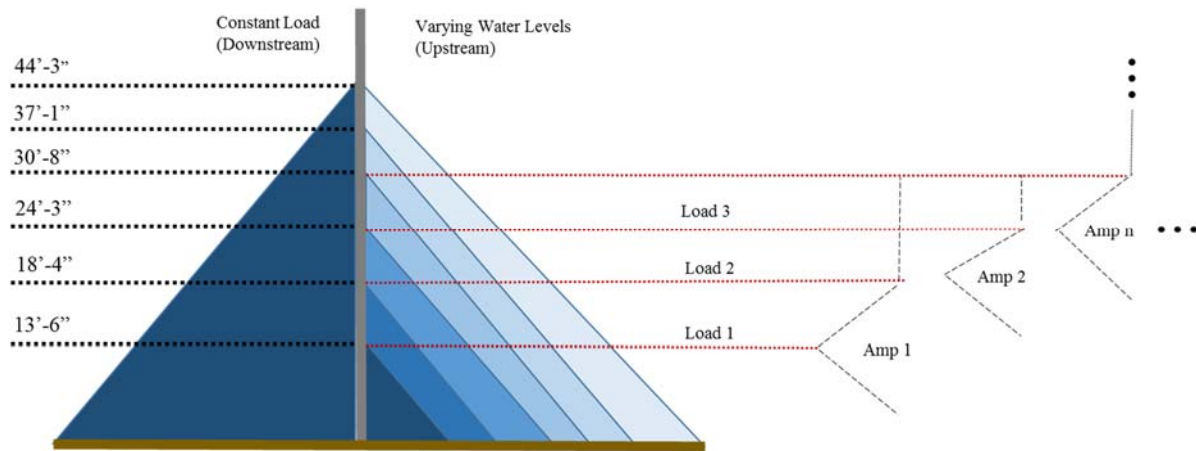


Figure 3. Hydrostatic Load Levels Used in Finite Element Analysis

3.1.2 Finite Element Model Analysis

The finite element analysis model calculates different stresses. Twenty-seven regions of high stress were identified on the gate, see Figure 4. Anomalies were identified and excluded from the fatigue analysis. Nodes are limited to one boundary condition which creates anomalies where nodes share multiple boundary conditions. Distorted elements, such as triangular elements near corners, also cause anomalies due to the geometry of the gate.

Each region of high stress was first assigned a category from the AASHTO LRFD Bridge Design Specifications (AASHTO, 2014;2015). The category identified the direction of stress for each section so that stress values could be collected. The stress values come from elements in the finite element model. Each element in a section provided two sets of data for every time-step in the cycle. The two data sets occur because a shell element has thickness, so one set of values is for the front of the element and the other is for the back.

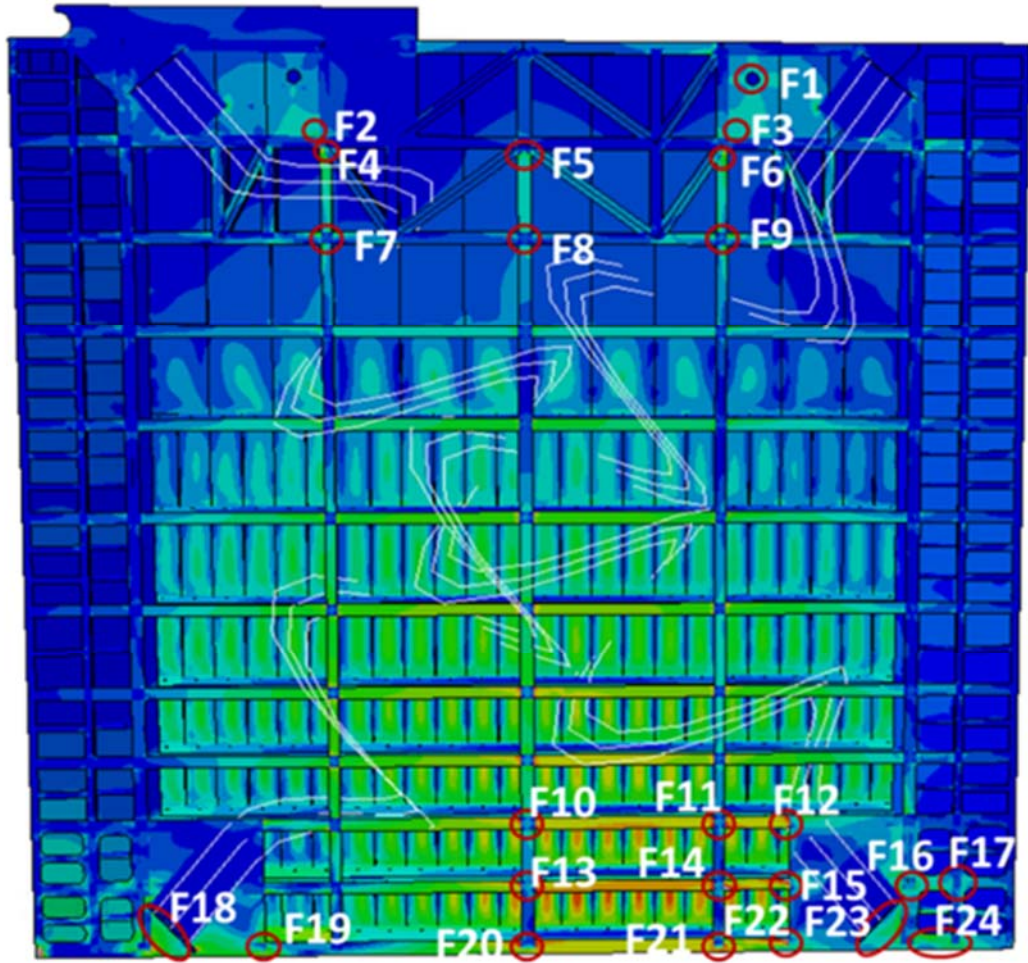


Figure 4. Identified Sections of High Stress in Finite Element Model

3.2 Data Analysis

Damage was calculated using Miner's Rule. Miner's Rule is a model for cumulative damage. Damage is the result of a cycle exceeding the fatigue threshold; the more cycles that exceed, the more damage that occurs. The finite element model gave stress data at a given time in the analysis. The reservoir counting procedure was used to determine the number of cycles for each applied stress range needed for Miner's total damage approach.

3.2.1 Miner's Rule

Miner's Rule is a cumulative damage approach used to evaluate fatigue performance in structural components. This approach calculates damage by equating it to the proportion of the number of cycles occurred to the number of cycles to failure for an applied stress range as shown in Equation 3-1.

$$\sum D_i = \sum \frac{n_i}{N_i} \quad \text{Equation 3-1}$$

where i is an applied stress range, D_i is the damage, n_i is the number of cycles, and N_i is the number of cycles to failure. The number of cycles to failure, N_i , is calculated using a constant determined by a section's category, A , and the applied stress range, $\Delta\sigma$, of a section. The equation for N_i is shown in Equation 3-2.

$$N_i = A(\Delta\sigma)^{-3} \quad \text{Equation 3-2}$$

The proportion of cycles is also known as the fatigue capacity. If the fatigue capacity is less than the fatigue threshold, no damage will occur due to fatigue. The fatigue threshold is a given value based on characteristics of the section and the category specified by AAASHTO LRFD Design Specifications (AASHTO, 2014;2015). The number of cycles at an applied stress range can be determined from the stress data acquired from a model by applying a counting procedure such as the rain-flow counting procedure or reservoir counting procedure.

3.2.2 Reservoir Counting

Reservoir Counting is a cycle counting procedure used to transform graphical data of stress time relationships into the number of cycles at a specific stress range. It is different from other cycle counting methods because it produces complete cycles rather than half-cycles (Maddow, 1991). The first step is to identify the highest peaks and rearrange the graph so that the highest

peaks are at the starting point and ending point of a new graph, see Figure 5. Visualize the new graph being filled with water and every local minimum is a drainable reservoir. The next step is to drain each reservoir individually and measure the height of the reservoir in stress. Each drain is a cycle and each height is a stress range therefore, the number of cycles at a stress range can be determined by adding drains with equal heights, see Figure 6. In this work, only one or two cycles occurred per section so this procedure was relatively simple.

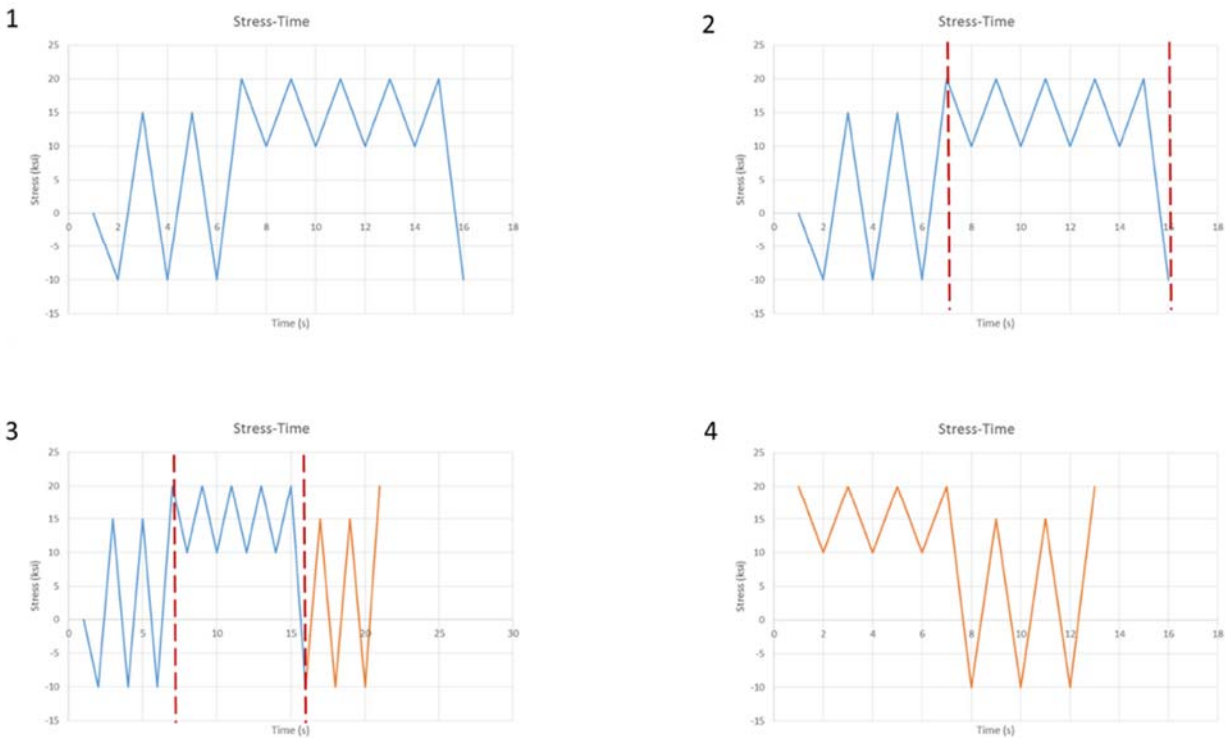


Figure 5. Rearrangement of Stress-Time Graph

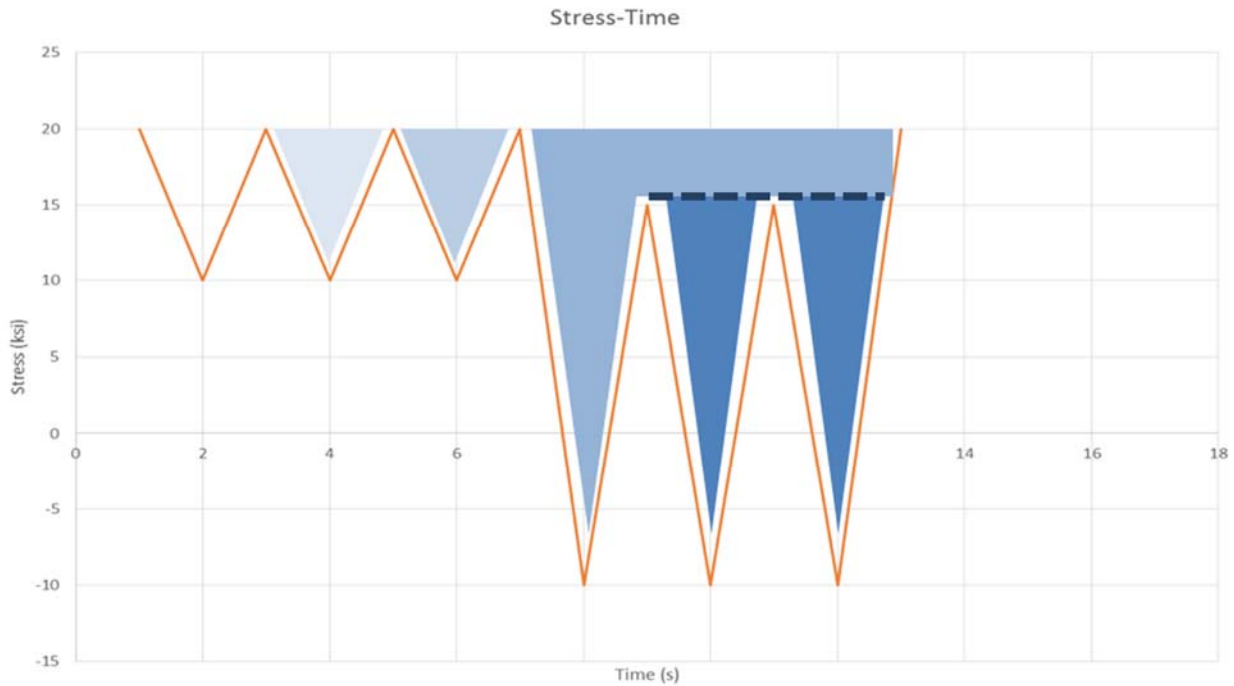


Figure 6. Visual Representation of Reservoirs

3.2.3 Application of Reservoir Counting Procedure

Since the finite element analysis produced two sets of data for every element in a section, it was simplified before applying the reservoir counting procedure. The two sets of data were averaged for all elements in a section; only the maxima of those two sets was used. For example, a section of three elements produces six columns of data, see Table 1(a). Three of these are a set and are averaged together, see Table 1(b). The averaged sets were plotted to visualize the reservoir, see Figure 7.

In this figure, the reservoir counting procedure has been used to find the applied stress range, $\Delta\sigma$, for one cycle. The smaller maximum was used for the reservoir height. The applied stress range was found for every section by plotting its stress contours and applying the reservoir counting procedure, see Figure 8.

Table 1. Visual Example of Data Collection for All Data and Average of Sets, (a) and (b) respectively.

SP1		SP5		SP1		SP5		SP1		SP5		Average					
152065				152066				152067				SP1		SP5			
X	Y	X	Y	X	Y	X	Y	X	Y	X	Y	X	Y	X	Y	X	Y
2	27.2138	2	27.8064	2	26.9946	2	27.6008	2	26.8167	2	27.4105			2	27.20876	2	27.80172
3	26.368	3	26.9398	3	26.145	3	26.7308	3	25.9624	3	26.5359			3	26.36516	3	26.93808
4	25.5232	4	26.0743	4	25.2966	4	25.8614	4	25.1089	4	25.6621			4	25.52274	4	26.07542
5	24.6804	5	25.2107	5	24.4501	5	24.994	5	24.2572	5	24.7902			5	24.68228	5	25.21474
6	23.8394	6	24.3491	6	23.6054	6	24.1284	6	23.4073	6	23.92			6	23.84366	6	24.35596
7	23	7	23.4891	7	22.7623	7	23.2644	7	22.559	7	23.0514			7	23.00666	7	23.4988
8	22.4716	8	22.9484	8	22.2332	8	22.7229	8	22.0284	8	22.5087			8	22.47922	8	22.95936
9	21.9437	9	22.408	9	21.7045	9	22.1817	9	21.4982	9	21.9663			9	21.95222	9	22.42026
10	21.416	10	21.868	10	21.1762	10	21.6409	10	20.9684	10	21.4243			10	21.42554	10	21.88154
11	20.8886	11	21.3283	11	20.6481	11	21.1004	11	20.4388	11	20.8826			11	20.89912	11	21.34316
12	20.3615	12	20.7889	12	20.1203	12	20.5601	12	19.9095	12	20.3411			12	20.373	12	20.805
13	19.8306	13	19.9391	13	19.2905	13	19.7111	13	19.0795	13	19.4924			13	19.54314	13	19.95668
14	18.7002	14	19.0899	14	18.4613	14	18.8627	14	18.2501	14	18.6442			14	18.7138	14	19.1089
15	17.8703	15	18.2412	15	17.6325	15	18.0148	15	17.4212	15	17.7966			15	17.88494	15	18.26166
16	17.0408	16	17.393	16	16.8041	16	17.1673	16	16.5927	16	16.9493			16	17.05648	16	17.41486
17	16.2117	17	16.5453	17	15.9762	17	16.3203	17	15.7646	17	16.1025			17	16.22846	17	16.56856
18	15.1895	18	15.5004	18	14.9584	18	15.2793	18	14.7498	18	15.0648			18	15.20684	18	15.5247
19	14.1678	19	14.4561	19	13.9412	19	14.2389	19	13.7356	19	14.0277			19	14.18576	19	14.48144
20	13.1466	20	13.4125	20	12.9246	20	13.1992	20	1.27E+01	20	12.9913			20	13.16522	20	13.43884
21	12.126	21	12.3695	21	11.9086	21	12.1601	21	11.709	21	11.9555			21	12.14526	21	12.39682
22	11.1058	22	11.3271	22	10.8931	22	11.1216	22	10.6967	22	10.9204			22	11.12578	22	11.35538
23	10.0036	23	10.2011	23	9.79938	23	10.0032	23	9.60975	23	9.80887			23	10.02357	23	10.22965
24	8.902	24	9.07579	24	8.70633	24	8.88543	24	8.52358	24	8.69819			24	8.92195	24	9.104598
25	7.80096	25	7.95116	25	7.61397	25	7.76844	25	7.4382	25	7.58829			25	7.820918	25	7.980182
26	6.70048	26	6.82722	26	6.52228	26	6.65217	26	6.35358	26	6.47918			26	6.720458	26	6.856412
27	5.60056	27	5.70395	27	5.43127	27	5.53662	27	5.26974	27	5.37084			27	5.620576	27	5.73327
28	4.46693	28	4.54644	28	4.31041	28	4.39058	28	4.15987	28	4.23578			28	4.486236	28	4.575144
29	3.33378	29	3.38952	29	3.1902	29	3.24524	29	3.05079	29	3.10152			29	3.352378	29	3.417562
30	2.20112	30	2.23321	30	2.07064	30	2.10059	30	1.94251	30	1.96809			30	2.219012	30	2.260536

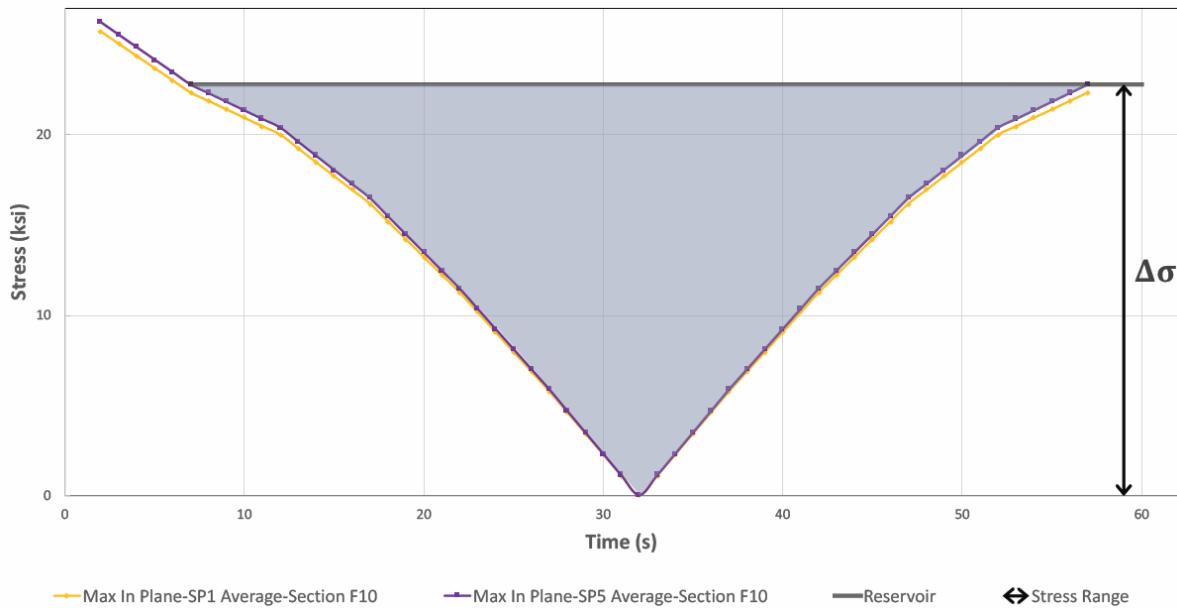


Figure 7: Application of reservoir counting procedure for the max in-plane stress history from Section F10

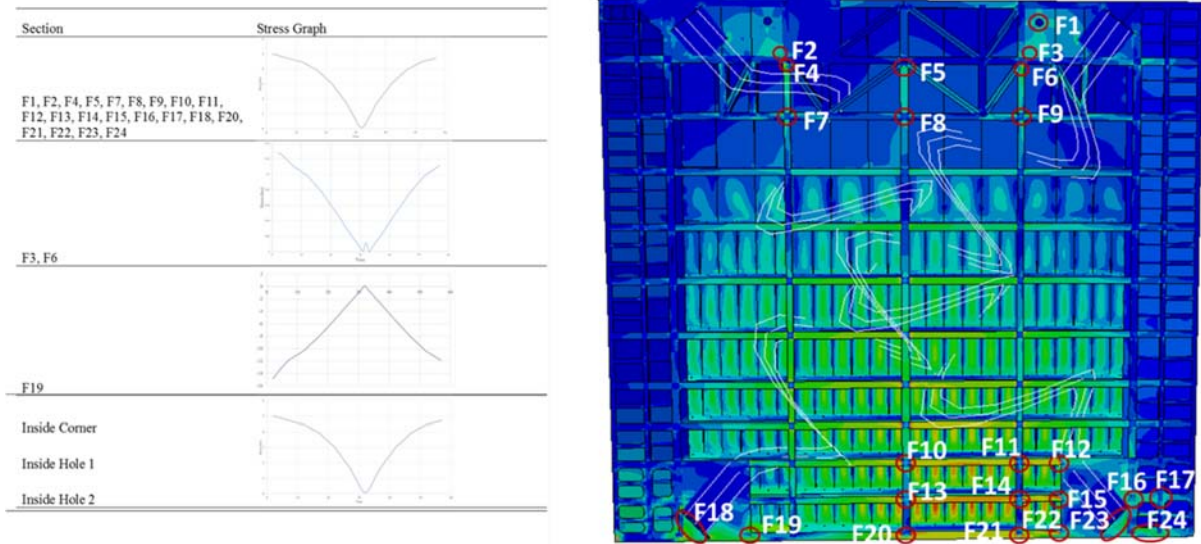


Figure 8. All Sections of High Stress and Corresponding Stress Graphs

3.2.4 Application of Miner's Rule

Miner's Rule, Equation 3-2, can be applied once the applied stress ranges for every section are found. The number of cycles to failure is a function of the applied stress range and a constant, A, given by the section's category classification (AASHTO, 2014;2015). Each section was divided into singular cycles for the applied stress range calculations so the number of cycles, n_i , was always one. This simplifies Equation 3-1 of Miner's Rule to damage equaling the inverse of the number of cycles to failure as shown in Equation 3-3.

$$\sum D_i = \sum \frac{1}{N_i} \quad \text{Equation 3-3}$$

The amount of damage to a section is the sum of the damage occurring in every cycle a section goes through. Some sections only had one cycle while others had two cycles. Damage only occurs if the amount of damage is higher than the fatigue threshold, given by the section's category classification in AASHTO. The procedures used to calculate damage can be condensed into Table

2. The highlighted section is the section with the most damage due to fatigue, see Figure 9. The sections without damage due to fatigue are not listed.

Table 2. Damage Results based on Application of Miner's Rule

Location	Category	Type	No. Cycles	$\Delta\sigma$	A (ksi ³)	Δf (ksi)	Nf (cycles)	Damage (N/Nf)	Total Damage Per Section
Section F7	E	7.1	1	5.945	1.10E+09	4.5	5.235E+06	1.910E-07	1.910E-07
Section F9	E	7.1	1	7.093	1.10E+09	4.5	3.082E+06	3.244E-07	3.244E-07
Section F10	E	7.1	1	22.732	1.10E+09	4.5	9.364E+04	1.068E-05	1.068E-05
Section F11	E	7.1	1	22.52	1.10E+09	4.5	9.631E+04	1.038E-05	1.038E-05
Section F12	E	7.1	1	21.584	1.10E+09	4.5	1.094E+05	9.141E-06	9.141E-06
Section F13	E	7.1	1	23.444	1.10E+09	4.5	8.537E+04	1.171E-05	1.171E-05
Section F14	E	7.1	1	23.301	1.10E+09	4.5	8.695E+04	1.150E-05	1.150E-05
Section F15	E	7.1	1	22.022	1.10E+09	4.5	1.030E+05	9.709E-06	9.709E-06
Section F16	E	7.1	1	9.807	1.10E+09	4.5	1.166E+06	8.574E-07	8.574E-07
Section F17	E	7.1	1	9.807	1.10E+09	4.5	1.166E+06	8.574E-07	8.574E-07
Section F20	E	7.1	1	22.411	1.10E+09	4.5	9.773E+04	1.023E-05	1.023E-05
Section F21	E	7.1	1	21.916	1.10E+09	4.5	1.045E+05	9.570E-06	9.570E-06
Section F22	E	7.1	1	19.854	1.10E+09	4.5	1.406E+05	7.114E-06	7.114E-06
Section Inside 1	D	1.5	1	12.534	2.20E+09	7	1.117E+06	8.950E-07	8.950E-07
Section Inside 2	D	1.5	1	10.37	2.20E+09	7	1.973E+06	5.069E-07	5.069E-07

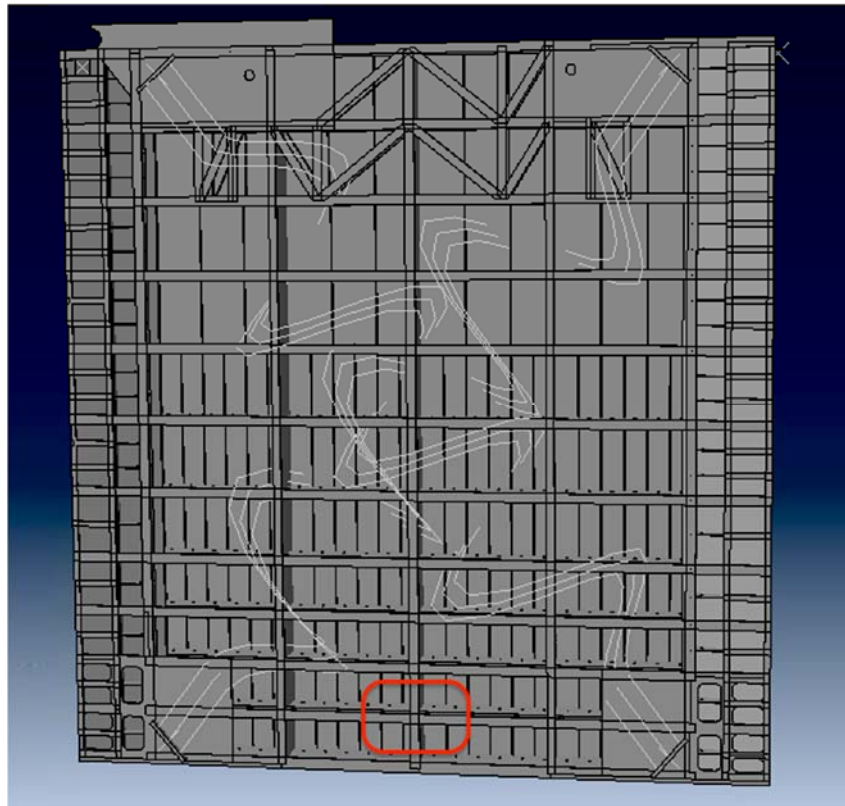


Figure 9. Miter Gate Locating Section F13

4. Results and Discussion

4.1 Results

Damage due to fatigue was measured by applying the reservoir counting procedure and Miner's Rule to the maximum stresses for each section of high stress that was identified using finite element modeling. This resulted in the section labeled F13 being the section with the most damage due to fatigue. Section F13 is located near the base of the miter gate, see Figure 9.

The resulting location of the section of highest fatigue is reasonable due to common knowledge of load resultants and the geometry of that section. The section has increasing tension forces being applied to it due to the hydrostatic pressures on the back of the gate. As the water level rises, the pressure on the bottom of the gate increases. The center is even more vulnerable because of its distance to a fixed body. The geometry classifies the section as a "transversely loaded welded attachment" according to AASHTO LRFD Design Specifications, see Figure 10. The transition radius of the plates assigns Category E on a scale from A-F. The scale refers to a sections ability to resist fatigue with Category A being the most resisting category. The thin plates welded together make this section the most critical section for damage due to fatigue.

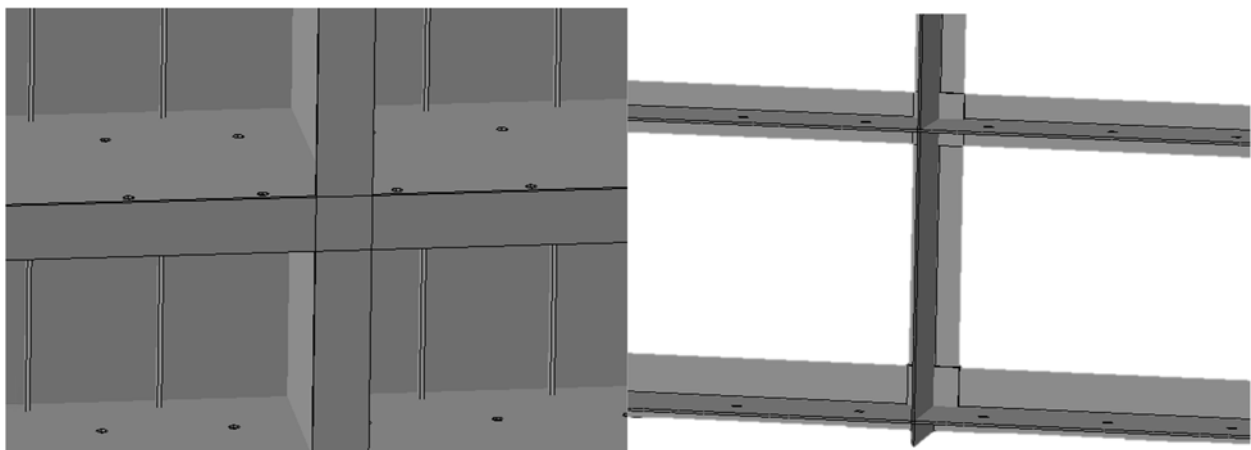


Figure 10. Detailed Geometry of the Front and Back of Section F13, (a) and (b) respectively

5. Conclusion

Determining the amount of damage that occurs on a lock gate is beneficial to the waterway transportation system. Unscheduled maintenance due to fatigue cracking is expensive and possibly preventable. Miner's Rule calculates damage by equating it to the fatigue capacity of a structural element. The fatigue capacity can be calculated using an applied stress range that can be found from a finite element analysis. In the future, an actual lock gate will be monitored so that these results can be validated. Organizations like the US Army Corps of Engineers can use this data to prevent unscheduled maintenance and get funding to prevent failures due to fatigue.

References

Arkansas State Highway and Transportation Department. (2015). *Size and Weight Laws*.

Retrieved from Arkansas Highways:

https://www.arkansashighways.com/highway_police/map21/Size_Weight.pdf

ASCE. (2017). *Inland Waterways*. American Society of Civil Engineers, Infrastructure Report Card.

Baker, M. M. (2004, August 20). As the Economy Sinks, 'Bush Doesn't Give a Dam'. *Executive Intelligence Review*.

Grier, D. V. (not sure). *The Declining Reliability of the U.S. Inland Waterway System*. ASCE, Institute for Water Resources. U.S. Army Corps of Engineers.

Maddow, S. J. (1991). *Fatigue Strength of Welded Structures* (Second Edition ed.). Cambridge, England: Abington Publishing.

USACE. (2013, August 30). *Navigation*. Retrieved April 2017, from US Army Corps of Engineers Headquarters: <http://www.usace.army.mil/Missions/Civil-Works/Navigation/>

WCSC. (2015). *Final Waterborne Commerce Statistics*. U.S. Army Corps of Engineer, Waterborne Commerce Statistics Center.